Kinetics and Catalysis, Vol. 43, No. 4, 2002, pp. 522–527. From Kinetika i Kataliz, Vol. 43, No. 4, 2002, pp. 566–571.
Original English Text Copyright © 2002 by Yan Liu, Zhanlin Xu, Tiexin Cheng, Guangdong Zhou, Junxia Wang, Wenxing Li, Yingli Bi, Kaiji Zhen.

Studies on Carbon Deposition on Hexaaluminate $LaNiAl_{11}O_{19}$ Catalysts during CO_2 Reforming of Methane[1]

Yan Liu*, Zhanlin Xu, Tiexin Cheng*, Guangdong Zhou*, Junxia Wang*, Wenxing Li*, Yingli Bi*, and Kaiji Zhen***

** Department of Chemistry, Jilin University, Changchun, 130023, P. R. China; e-mail:byl@mail.jlu.edu.cn*

*** Department of Chemistry, Siping normal college, Siping, 136000, P. R. China*

Received May 21, 2001

Abstract—The amount of carbon deposited on hexaaluminate $LaNiAl_{11}O_{19}$ catalyst in CH_4 decomposition and CO_2 reforming of methane was determined by means of thermogravimetric analysis (TGA). The properties of carbon formed on the catalysts were characterized by X-ray photoelectron spectroscopy (XPS), temperature-programmed CO_2 reaction (TPR-CO_2), and temperature-programmed oxidation (TPO) techniques. The experimental results showed that hexaaluminate $LaNiAl_{11}O_{19}$ catalyst possessed high resistance to carbon deposition in CO_2 reforming of methane to synthesis gas at high temperatures, and CO_2 played an important role in eliminating carbon during the reaction. At least two forms of the deposited carbon, graphite and carbide, were produced during methane reforming with CO_2.

INTRODUCTION

Catalytic reforming of methane with CO_2 to synthesis gas has attracted considerable attention in the past three decades [1, 2]. This reaction has environmental importance since both CH_4 and CO_2 contribute to the greenhouse effect. They are also starting materials for producing synthesis gas, which may fulfill the requirement of many synthesis processes in the chemical industry. In addition, since the synthesis gas produced by this reaction possesses a low H_2/CO ratio, it is more suitable for the Fischer–Tropsch synthesis to produce liquid hydrocarbons and oxygen containing derivatives.

Generally, factors causing deactivation of the catalyst are carbon deposition, sintering of active sites, and solid-phase reactions of active metals with the support. Among them, carbon deposition is the most serious problem. According to thermodynamic calculation, CO_2 reforming of methane is much more prone to cause carbon deposition than steam reforming because of its low H_2/CO ratio in the reaction products. Several types of carbon were detected by Sacco *et al.* [3] and Jablonski *et al.* [4], and the origin of the carbon formation has also been investigated. It is reported that CH_4 decomposition and CO disproportionation are the main routes to carbon deposition, and their relative amount depends on reaction conditions.

To date, a number of studies have been focused on the development of catalysts that show high activity and stability and on reducing the amount of deposited carbon in methane reforming with CO_2 [5, 6]. It is found that carbon deposition depends on the choice of metal. Noble metals, such as Ru, Rh, and Ir supported on Eu_2O_3, MgO, and Al_2O_3 exhibit high ability to suppress carbon formation [7, 8]. On the contrary, on most of the group VIII transition metals, especially Ni-based catalysts, carbon deposition is facile.

The effect of the nature of support on carbon deposition has also been emphasized in recent years. It has been suggested that carbon deposition may be suppressed when the metal is supported on metal oxides with strong Lewis basicity [9]. Moreover, it is also plausible that carbon deposition is more closely related to the catalyst structure. Chen and Ren have convincingly shown that, in CO_2 reforming of methane over a Ni/Al_2O_3 catalyst, carbon deposition may markedly be suppressed when $NiAl_2O_4$ is formed during the pretreatment procedure [10, 11]. The catalytic properties of NiO/MgO have also been investigated [12]. It has been found that the NiO–MgO solid solutions formed in NiO/MgO catalyst can stabilize small Ni crystallites and enhance catalyst lifetime by decreasing carbon formation. We have also reported two series of hexaaluminates $ANiAl_{11}O_{19-\delta}$ (A = Ca, Sr, Ba, and La) and $LaNi_yAl_{12-y}O_{19-\delta}$ (y = 0.3, 0.6, 0.9, and 1.0) as new catalysts for CO_2 reforming of methane to synthesis gas, in which the active component Ni is inlayed in the hexaaluminate lattices to substituted a part of Al ions [13, 14]. Of all hexaaluminates, $LaNiAl_{11}O_{19}$ exhibited high catalytic activity and stability, providing over 95.4 and 96.7% conversion of CH_4 and CO_2, respectively, which remained unchanged for 18 h of time-on-stream.

The aim of this paper is to find the reason for the low amount of carton deposited at 800° over hexaaluminate $LaNiAl_{11}O_{19}$ in methane reforming with CO_2.

[1] This article was submitted by the authors in English.

0023-1584/02/4304-0522$27.00 © 2002 MAIK "Nauka / Interperiodica"

EXPERIMENTAL

Hexaaluminate $LaNiAl_{11}O_{19}$ catalyst was prepared by the decomposition of nitrates and calculations at high temperature as reported previously [13, 14]. The amount of carbon deposited on hexaaluminate $LaNiAl_{11}O_{19}$ catalyst was determined by using a thermogravimetric analyzer (Perkin-Elmer TGA7). The catalyst was first reduced in H_2 at 900°C for 0.5 h in a fixed-bed continuous flow reactor and then cooled down to 25°C and was exposed to the reaction conditions at 500, 600, 700, 800 °C for 2 h, respectively. The weight change of the sample was simultaneously recorded. The molar composition of reactant mixture was CH_4/Ar = 1/3 for methane decomposition, CO/Ar = 1/3 for CO disproportionation, and CO_2/CH_4/Ar = 1/1/2 for CO_2/CH_4 reforming. The total flow rate was 40 ml/min.

The samples characterized by TPR-CO_2 and TPO were treated according to the conventional procedure of TG measurement. The feed gas was switched to Ar gas for 10 min for purging, and then the reactor was quickly cooled down to room temperature, followed by TPR-CO_2 (50% CO_2/Ar) or TPO (10% O_2/Ar) gas characterization. Highly pure Ar (99.99%), CO_2 (99.98%), and H_2 (99.95%) were used. In each case the mixture gas flow rate was 40 ml/min. The temperature was raised from room temperature to 800°C at a heating rate of 20°C/min, The effluent gas was analyzed by a gas chromatograph (Shimadzu GC-8A) equipped with a thermal conductivity detector (TCD).

The deposited carbon on hexaaluminate $LaNiAl_{11}O_{19}$ catalyst was characterized by X-ray photoelectron spectroscopy (XPS) (V. G. ESCA Mark II) using AlK_α radiation; the analyses were operated at a pass energy of 50 eV and a step size of 0.05 eV. The peak of the contaminated carbon at 284.6 eV was used as internal standard. The sample probe was transferred using a glove box with highly pure N_2 to prevent the samples from contacting atmospheric O_2 and H_2O.

TEM images of deposited carbon were taken by means of a HITACHI-8100IV operated at 200 KV. The sample of deposited carbon was treated with 3M HNO_3 and then dispersed by supersonic waves in an aqueous surfactant solution before being mounted on a Cu grid for TEM observation.

The metallic nickel particle size was calculated by the Scheerer formula with fwhm of the principal peak, which was determined by XRD (Shimadzu XD-3A diffractometer) at a scanning rate of 1°C/4 min using Ni-filter and CuK_α radiation, at 30 kV and 20 mA.

RESULTS AND DISCUSSION

1. Carbon Formation during CH_4 Reforming with CO_2

There are two routes of carbon deposition in the CO_2 reforming of CH_4 to synthesis gas:

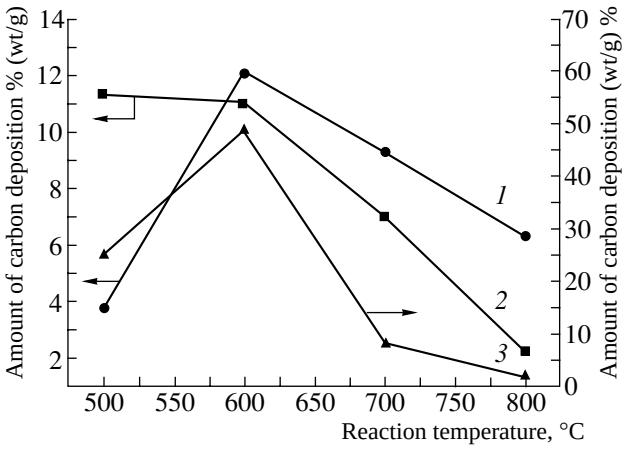

Fig. 1. Variation of carbon deposition with the reaction temperature: (*1*) CH_4 decomposition, (*2*) CO disproportionation, and (*3*) CO_2 reforming of CH_4.

CO disproportionation: $2CO = C + CO_2$ (ΔH = –170 KJ/mol),

CH_4 decomposition: $CH_4 = C + 2H_2$ (ΔH = 74 KJ/mol).

A summary of the amount of carbon deposition in the CO_2 reforming of CH_4, CH_4 decomposition, and CO disproportionation reaction at different temperatures after 2 h is shown in Fig. 1. The amount of carbon formed in the first two reactions increases with an increase in temperature below 600°C, then decreases above this temperature, and similar shapes of the two profiles are found as well. However, in the last reaction a change in the amount of carbon with an increase in the reaction temperature is different from the former two. Thermodynamic analysis shows that this reaction is exothermic. Thus, the equilibrium constantly decreases with an increase in reaction temperature. In other words, at high temperatures, CO disproportionation is not a dominant route of carbon deposition. So in this work, the characters of CH_4 decomposition and CO_2 reforming CH_4 were mostly studied.

Figures 2a and 2b show rates of carbon formation with time-on-stream at various temperatures. It can be seen from Fig. 2a that the rates of carbon formed in CH_4 decomposition rapidly increase with the time-on-stream to 0.3 and 0.47 g C (g cat)$^{-1}$ h^{-1} after 50 min at 500 and 600°C, respectively. However, the rates slowly drop to 0.1 and 0.04 g C (g cat)$^{-1}$ h^{-1} under the same conditions at 700 and 800°C, respectively. Figure 2b shows that the rates of carbon formed in reforming of methane rapidly drop with the time-on-stream to less than 0.03 g C (g cat)$^{-1}$ h^{-1} after 50 min at various reaction temperatures.

According to the thermodynamics, the amount of carbon deposited by CH_4 decomposition should increase with an increase in temperature. However, Fig. 2a indicates that below 600°C, the amount of deposited carbon obeys the thermodynamic rule, and,

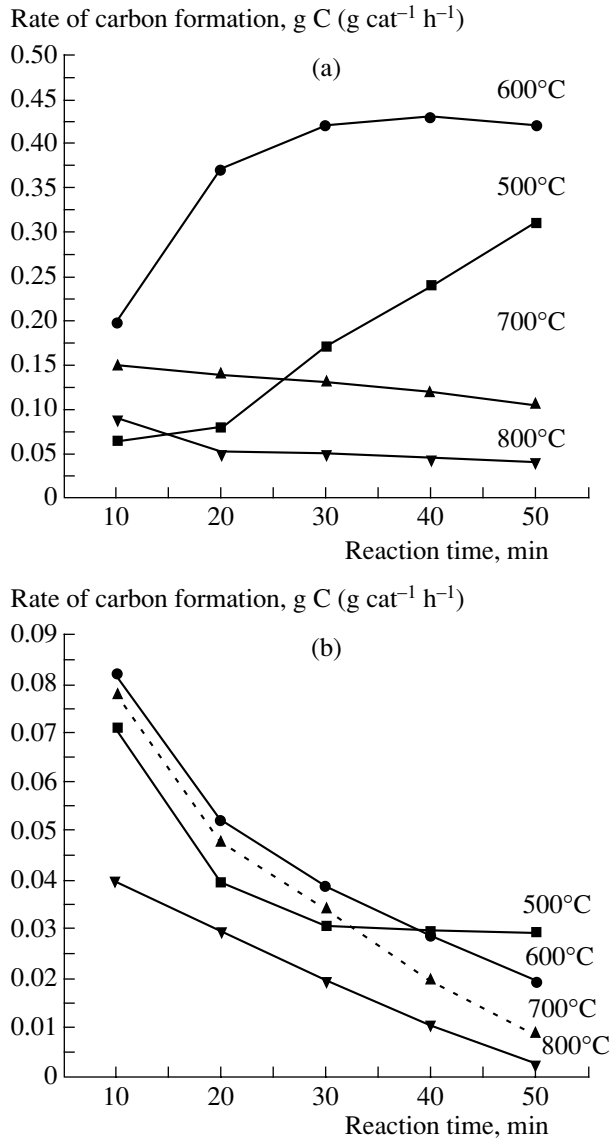

Fig. 2. (a) Rate of carbon formation vs. reaction time during CH_4 decomposition at different temperatures. (b) Rate of carbon formation vs. reaction time during CO_2 reforming of CH_4 at different temperatures.

in the range 600–800°C, it monotonously decreases with the temperature. The reason for the difference in the carbon deposition rates between different temperature ranges might be due to the difference in the carbon formation mechanism. The carbon forms produced at low temperatures were active, but disappeared at a high temperature. Figure 2b shows that the rate of carbon formation gradually drops with time-on-stream at high temperatures. In the meantime, it also indicates that the carbon deposition is not the reason for the catalyst deactivation. Inactive carbon is the direct reason for the catalyst deactivation due to its interaction with the catalyst [15].

2. TEM Measurements

It is possible to determine the particle size distribution of Ni^0 from the TEM images in Fig. 3, which give an average particle size of 45 nm. This value is in a reasonable agreement with the result of XRD slow scanning technique, which gives 48.7 nm. The particle size of nickel does not change after 2-h reaction indicating that the Ni ions inlayed in the hexaaluminate lattices are extremely stable and resistant to sintering. The reason for this phenomenon is that the strong interaction between the small Ni crystallites and the hexaaluminate makes the catalyst relatively stable toward sintering and carbon deposition [16].

The TEM images of the $LaNiAl_{11}O_{19}$ catalyst provided clear evidence for carbon formation during the reaction under consideration at different temperatures. At 600°C (Fig. 3a), the formed carbon existed in the form of fluffy stick covering part of the active centers; and at 800°C (Fig. 3b) in the form of filamentous whiskers. Their size is approximately 50 nm in diameter, have a hollow core; and on the top of filamentous whisker the black point can be found, which is metallic nickel. Carbon atoms deposited in this form on the backside of metal crystallite. That is, the filamentous whisker was formed via deposition of carbon on the back of the nickel particle. The driving force for this diffusion process is considered to be heat generated by exothermic surface processes, such as CO adsorption and disproportionation [19].

The authors would like to point out that the TEM profiles clearly indicate the existence of some type of nanocarbon tube (NCT) produced during CH_4 decomposition and methane reforming with CO_2, respectively. About the details we will depict in a followed report.

3. XPS Measurements

It is known that CH_4 decomposition and CO disproportionation proceed as two important reactions in CO_2 reforming of methane and are supposed to be possible routes to deposited carbon. It has been reported that the reactive surface carbon originates from CH_4 decomposition. In contrast, it has also been claimed that the accumulated carbon species are originated from CO_2 [15]. In this study, the surface carbon species on the hexaaluminate $LaNiAl_{11}O_{19}$ catalyst may form in CH_4 decomposition and CO_2 dissociation were investigated by XPS technique. It has been verified by XPS that no surface deposited carbon was detected on the catalyst surface after CO_2 dissociation at high temperature. It is found from Fig. 4 that two kinds of deposited carbon were formed during CH_4 reforming with CO_2. The peak at 282.96 eV can be attributed to carbide carbon and the peak at 284.93 eV to graphitic carbon. The XPS data of carbon species on catalyst were discussed in [17, 18]. Compared with the results of Tables 1 and 2, on the surface of the hexaaluminate $LaNiAl_{11}O_{19}$ catalyst, the amount of graphitic carbon is higher than that of car-

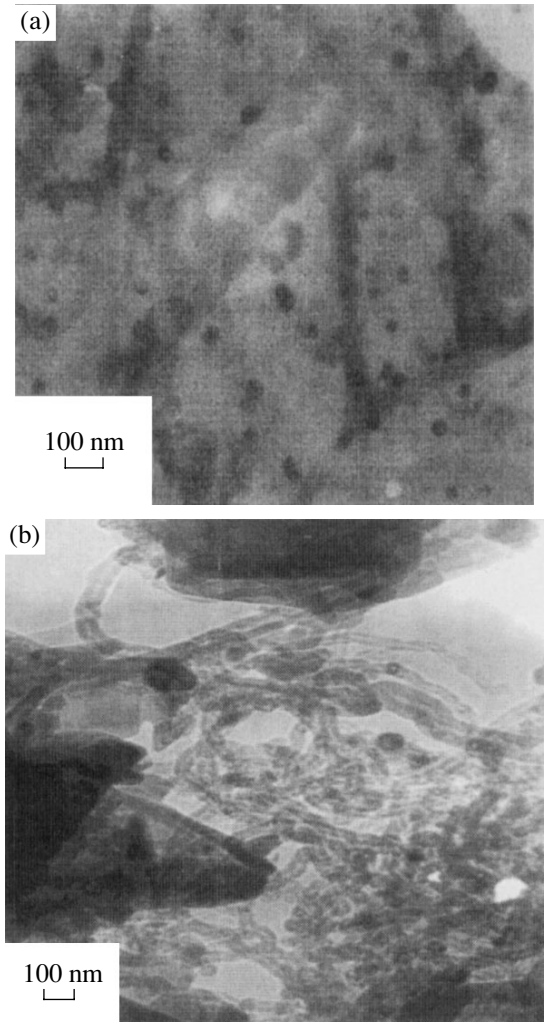

Fig. 3. TEM micrograph (50 × 1000): (a) after reaction at 600°C and (b) after reaction at 900°C.

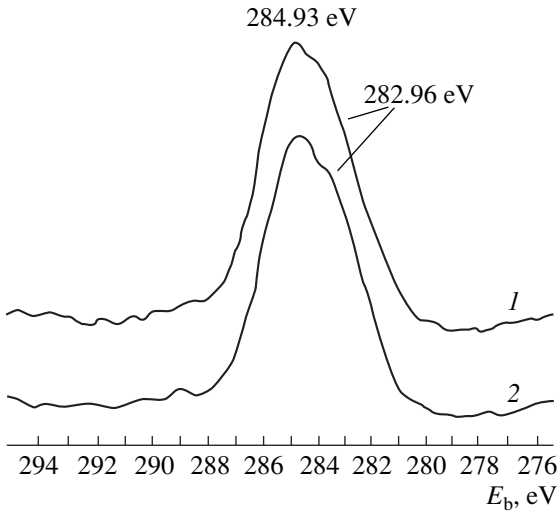

Fig. 4. XPS spectra of C1*s* in surface phase of hexaaluminate $LaNiAl_{11}O_{19}$ at 700°C after (*1*) CO_2 reforming of methane and (*2*) CH_4 decomposition.

bide carbon during the CH_4 reforming reaction. This can be explained from the viewpoint of surface segregation. On the other hand, carbide carbon exists in layers of coke, which may be divided into different types according to the degree of metal-to-carbon or carbon-to-carbon bonding. Layers of CH_x (*x* varied between 1 and 3 depending on the origin and history of the carbon deposition conduction) are on the Ni_3C. Active carbon is above the CH_x layers. Nickel carbide, CH_x and active carbon compose carbide carbon. All of them can be eliminated under suitable conditions.

4. Temperature-Programmed Oxidation

Figures 5a and 5b show the TPO profiles of the carbon deposited on the $LaNiAl_{11}O_{19}$ catalyst after CH_4 decomposition and CO_2 reforming of methane at different temperatures. In all TPO profiles, a peak in a temperature range of 450–600°C and another peak in a range of 650–950°C are found. No CO was formed during TPO experiments, while only traces of H_2O were detected. The above-mentioned results indicated that two forms of deposited carbon exist, and some deposited carbon species still contained hydrogen. In the TPO profiles of carbon deposited during CH_4 decomposition also shown in Table 2, the ratio of the peaks at low temperature are much higher than that of peaks at high temperature, and the low temperature peak decreases with an increase in the temperature. In contrast, the area ratio of peaks at high temperature changes slightly at all temperatures. In the TPO profiles of CO_2 reforming of methane, the area ratios of peaks at low temperatures are the same as that of peaks at high temperatures. The area ratio of peak at low temperatures from CO_2 reforming of methane is much smaller than that from CH_4 decomposition under the same reaction conditions, indicating that carbon formed during the CH_4 decomposition is active, and can be partly eliminated during CO_2 reforming of methane. We assumed that this type of carbon might be carbide. Otherwise, the graphitic carbon was a predominant form of the deposited carbon at high temperatures.

The difference in the oxidation ability of carbon deposited by CH_4 decomposition and CO_2 reforming of methane indicates that CO_2 played an important role in suppressing carbon deposition during the reaction. The experimental results also showed that the ability of CO_2

Table 1. Relative content of C_g and C_c on surface of $LaNiAl_{11}O_{19}$ at 700°C measured by XPS

Reaction	C_g, %	C_c, %
CH_4 decomposition	52.8	47.2
CO_2 reforming CH_4	61.5	38.5

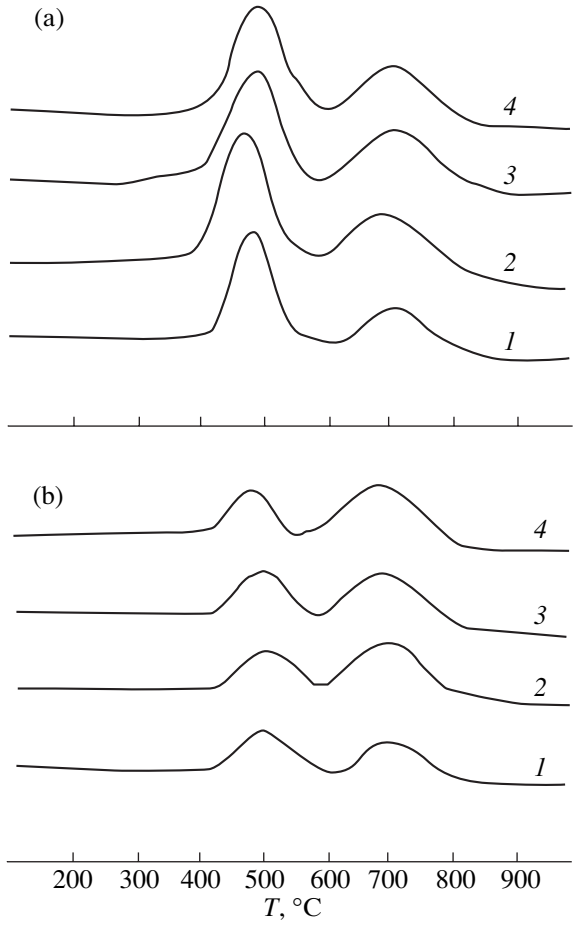

Fig. 5. (a) TPO profiles of deposited carbon during CH_4 decomposition at different temperatures: (*1*) 500°C, (2) 600°C, (*3*) 700°C, and (*4*) 800°C. (b) TPO profile of deposited carbon during CO_2 reforming of methane at different temperatures: (*1*) 800°C, (*2*) 700°C, (*3*) 600°C, and (*4*) 500°C.

to eliminate carbon deposition might be enhanced by raising reaction temperature.

5. Carbon Elimination by CO_2

It is found from Fig. 6 that CO_2 exhibited high catalytic activity in eliminating carbon deposited in CH_4 decomposition at different temperatures over hexaaluminate $LaNiAl_{11}O_{19}$ catalyst, and the activity increased with raising temperature. All the carbon deposited on the catalyst could be eliminated easily and completely at suitable temperatures. This is the reason for that the high resistance to carbon deposition and stability of the hexaaluminate $LaNiAl_{11}O_{19}$ catalyst is preserved. In the meantime, we observed that the peak of carbon eliminated by CO_2 increases with an increase in CH_4 decomposition temperature. This indicates that the composition of carbon deposited by CH_4 decomposition at high temperatures is more difficult to eliminate than that at low temperatures. The intensity of TPR-CO_2 peaks is also different at different CH_4 decomposition temperatures. This indicates that the content of active carbon produced during CH_4 decomposition is higher at low temperatures than at high temperatures. The surface inactive carbon was not easily eliminated with CO_2 and needed higher temperatures. Therefore, CH_4 was dissociated into carbide carbon, and was easily transformed into graphitic carbon with raising temperature. The graphitic carbon was the main form of the deposited carbon.

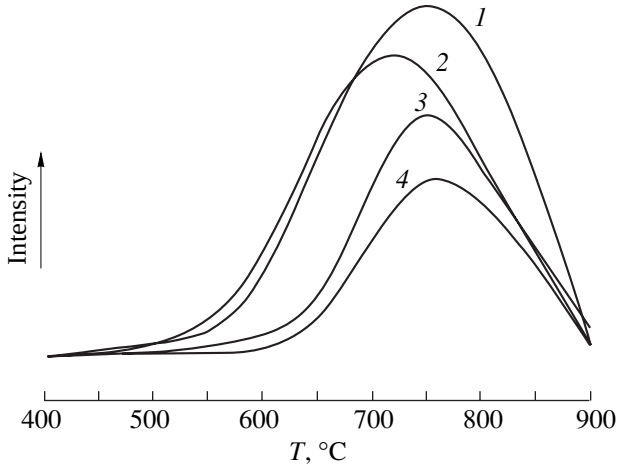

Fig. 6. TPR-CO_2 profiles of deposited carbon during CH_4 decomposition at different temperatures, (*1*) 600, (*2*) 500, (*3*) 700, and (*4*) 800°C, respectively.

Table 2. Relative content of deposited carbon on $LaNiAl_{11}O_{19}$ measured by TPO

Reaction temperature, °C	CH_4 decomposition		CO_2 reforming CH_4	
	C_c, %	C_g, %	C_c, %	C_g, %
500	66.3	33.7	51.2	48.8
600	63.6	36.4	44.5	55.5
700	60.2	39.8	41.8	58.2
800	59.1	40.9	38.6	61.4

CONCLUSIONS

The reduced hexaaluminate $LaNiAl_{11}O_{19}$ exhibited significant catalytic activities for both CH_4 decomposition and CO_2 carbon elimination, and the catalytic activities increased with an increase in the reaction temperature. Carbon deposited on the catalyst was produced by CH_4 decomposition in CO_2 reforming of methane. The carbon deposition could be suppressed at a suitable CH_4/CO_2 ratio and reaction conditions. There were two kinds of deposited carbon from produced in CH_4 decomposition during CO_2 reforming of methane. Carbide carbon was unstable and could be easily transferred into graphite like carbon, which was the main carbon form produced over this type of catalyst. It is

very important to quantitatively determine the dominant factors of carbon deposited on the catalyst.

ACKNOWLEDGMENTS

The authors gratefully acknowledge the support of this work from NNSF China (29973012).

REFERENCES

1. Fujimoto, K., *Stud. Surf. Catal.*, 1994, vol. 81, p. 73.
2. Richardson, J.T., and Paripatyadar, S.A., *Appl. Catal. A*, 1990, vol. 61, p. 293.
3. Sacco, A., Geurts, F.W.A.H., Jablonski, G.A., *et al. J. Catal.*, 1989, vol. 119, p. 332.
4. Nolan, P.E., Lynch, D.C., and Cutler, A.H., *Carbon*, 1994, vol. 32, p. 477.
5. Erdonhelyi, A., Cserenyi, J., and Solymosi, F., *J. Catal.*, 1993, vol. 141, p. 287.
6. Bradford, M.C.J. and Vannice, M.A., *Catal. Rev.–Sci. Eng.*, 1999, vol. 4, no. 1, p. 1.
7. Solymosi, F., Kustan. Gy., and Erdohelyi, A., *Catal. Lett.*, 1991, vol. 11, p. 149.
8. Qin, D. and Lapszewicz, J., *Catal. Today*, 1994, vol. 21, p. 551.
9. Yamazaki, O., Nozake, T., Omata, K., and Frjimoto, K., *Catal. Lett.*, 1992, vol. 19, p. 53.
10. Chen, Y.G. and Ren, J., *Catal. Lett.*, 1994, vol. 29, p. 39.
11. Bhattacharyya, A. and Chang, V.W., *Stud. Sruf. Sci. Catal.*, 1994, vol. 88, p. 207.
12. Gadalla, A.M. and Sommer M.E., *J. Am. Ceram. Soc.*, 1989, vol. 72, p. 683.
13. Zhanlin Xu, Ming Zhen, Yingli Bi, and Kaiji Zhen, *Catal. Lett.*, 2000, vol. 64, p. 157.
14. Zhanlin Xu, Ming Zhen, Yingli Bi, and Kaiji Zhen, *Appl. Catal. A*, 2000, vol. 198, p. 267.
15. Tsipouriari, V.A., Efstthiou, A.M., Zhang, Z.L., and Verykio, X.E., *Catal. Today*, 1994, vol. 21, p. 579.
16. Bhattacharyya, A. and Chang, V.W., *Stud. Surf. Sci. Catal.*, 1994, vol. 88, p. 207.
17. Wang, S.B. and Lu. G.Q., *Appl. Catal. A*, 1998, vol. 169, p. 271.
18. Lu Yong, Yu Changchun, Liu Yu, *et al. Chem. Lett.* 1997, vol. 6, p. 515.
19. Bradford, M.C.J. and Vannice, M.A., *Catal. Rev.*, 1999, vol. 41, p. 1.